Chinese Chemical Letters 36 (2025) 110223

Contents lists available at ScienceDirect

Chinese Chemical Letters

journal homepage: www.elsevier.com/locate/cclet

Persistent luminescence encoding for rapid and accurate oral-derived bacteria identification

Chaohui Zheng[a,1], Jing Xi[b,1], Shiyi Long[b], Tianpei He[b], Rui Zhao[b], Xinyuan Luo[a], Na Chen[b,*], Quan Yuan[a,b,c,*]

[a] The Second Affiliated Hospital of Fujian Medical University, Quanzhou 362000, China
[b] Renmin Hospital of Wuhan University, College of Chemistry and Molecular Sciences, Institute of Molecular Medicine, School of Microelectronics, Wuhan University, Wuhan 430072, China
[c] Molecular Science and Biomedicine Laboratory (MBL), State Key Laboratory of Chemo/Biosensing and Chemometrics College of Chemistry and Chemical Engineering, Hunan University, Changsha 410082, China

ARTICLE INFO

Article history:
Received 28 May 2024
Revised 3 July 2024
Accepted 5 July 2024
Available online 6 July 2024

Keywords:
Oral microorganisms
Persistent luminescent nanoprobes
Optical sensing array
Fingerprint physicochemical properties
Linear discriminant analysis

ABSTRACT

The dysbiosis of oral microbiota contributes to diseases such as periodontitis and certain cancers by triggering the host inflammatory response. Developing methods for the immediate and sensitive identification of oral microorganism is crucial for the rapid diagnosis and early interventions of associated diseases. Traditional methods for microbial detection primarily include the plate culturing, polymerase chain reaction and enzyme-linked immunosorbent assay, which are either time-consuming or laborious. Herein, we reported a persistent luminescence-encoded multiple-channel optical sensing array and achieved the rapid and accurate identification of oral-derived microorganisms. Our results demonstrate that electrostatic attractions and hydrophobic-hydrophobic interactions dominate the binding of the persistent luminescent nanoprobes to oral microorganisms and the microbial identification process can be finished within 30 min. Specifically, a total of 7 oral-derived microorganisms demonstrate their own response patterns and were differentiated by linear discriminant analysis (LDA) with the accuracy up to 100% both in the solution and artificial saliva samples. Moreover, the persistent luminescence encoded array sensor could also discern the microorganism mixtures with the accuracy up to 100%. The proposed persistent luminescence encoding sensor arrays in this work might offer new ideas for rapid and accurate oral-derived microorganism detection, and provide new ways for disease diagnosis associated with microbial metabolism.

Periodontitis, as one of the most prevalent inflammatory diseases of the oral cavity, not only compromises the integrity and function of periodontal tissue but also impacts on the course and pathogenesis of a number of systemic diseases, such as cardiovascular disease, Alzheimer, type-2 diabetes and certain cancers [1–5]. Recently, it has been widely recognized that the dysbiosis of oral microbiota contributes to periodontitis by triggering the host inflammatory response [6,7]. To this end, having a dynamic and accurate view of oral microbiota offers great potential in the disease early warning and provide auxiliary ways for the exploration of disease mechanisms [8–10]. However, the oral biological samples are typically within various components which might bring about background signal, and the species and concentrations of the oral microorganism are dynamically changing. It still remains a grand challenge to discriminate and identify the evolving oral microorganisms in real-time with high signal to noise ratio and accuracy. Traditional methods for microbial detection primarily include plate culturing, polymerase chain reaction and enzyme-linked immunosorbent assay, which are either time-consuming or laborious [11–19]. Therefore, developing methods for the immediate and sensitive identification of oral microorganism is crucial for the rapid diagnosis and early interventions of periodontitis.

Optical sensors have garnered significant attention in the field of point-of-care detection due to its high sensitivity, rapid response and portability [20–27]. Long afterglow phosphorescent materials which own the distinct persistent luminescent optical property have drawn great attentions. By collecting the persistent luminescence signals of long afterglow phosphorescent materials after removing the external excitation, the background fluorescence

* Corresponding authors.
E-mail addresses: chenna0804@whu.edu.cn (N. Chen), yuanquan@whu.edu.cn (Q. Yuan).
[1] These authors contributed equally to this work.

https://doi.org/10.1016/j.cclet.2024.110223
1001-8417/

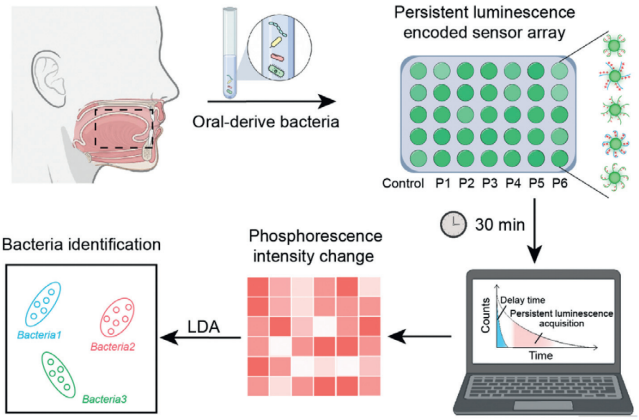

Scheme 1. Schematic illustration of the persistent luminescence encoded sensor array based on Zn_2GeO_4:Mn nanorods for rapid and accurate oral bacteria identification.

interference encountered in complex oral biological samples can be effectively eliminated [28–31]. With this intrinsic optical property, persistent luminescence sensors (PLNP) based optical sensors are capable of achieving the rapid and sensitive detection of oral-derived microorganism [32,33]. Sensor array, mimicking the mammalian olfactory and gustatory sensory systems, enable the identification of oral microorganisms through fingerprint recognition [34–40]. Developing persistent luminescence encoding sensor arrays offers excellent ideas for rapid and accurate oral-derived microorganism detection, and might pave the ways for disease diagnosis associated with microbial metabolism.

It has been widely validated that the microorganism can be efficiently and selectively identified by the fingerprint physicochemical properties. Hence, by rational design of the persistent luminescent nanoprobes with different physicochemical properties, the oral-derived microorganisms can be efficiently recognized and differentiated. Herein, we report a persistent luminescence-encoded multiple-channel optical sensing array and achieved the rapid and accurate identification of oral-derived microorganisms (Scheme 1). To be specific, Zn_2GeO_4:Mn (ZGO:Mn) as a kind of persistent luminescence nanomaterials was selected as the research model. Different nanoprobes with distinct charges and hydrophilicity were prepared by modifying different organic ligands on the surface of persistent luminescence nanoparticles (PLNPs) ZGO:Mn. Our results indicate that electrostatic attractions and hydrophobic-hydrophobic interactions dominate the binding of the nanoprobes to oral microorganisms. Seven oral-derived or oral diseased associated microorganisms demonstrate their own response patterns and can be differentiated by linear discriminant analysis (LDA) with accuracy up to 100% both in the solution and the complex artificial saliva samples. Moreover, the persistent luminescence encoded sensor array could also discern the microorganism mixtures both in the solution and artificial saliva samples with the accuracy up to 100%. It is worth mentioning that the microbial identification process can be finished within 30 min, much faster than the traditional methods for microbial detection including plate culturing (2–7 days) and polymerase chain reaction (6–8 h) [19,41]. Overall, the proposed persistent luminescence encoded sensor array strategy shows great potential for fast and accurate point-of-care test for microbial identification.

Persistent luminescent sensors have attracted numerous attentions owing to the intrinsic advantages including background-free detection and high signal-to-noise ratio [42–44]. As a proof of concept, herein we adopt the ZGO:Mn nanorods as persistent luminescent sensor model to explore the viability in oral bacterial detection. Specifically, ZGO:Mn nanorods were firstly prepared ac-

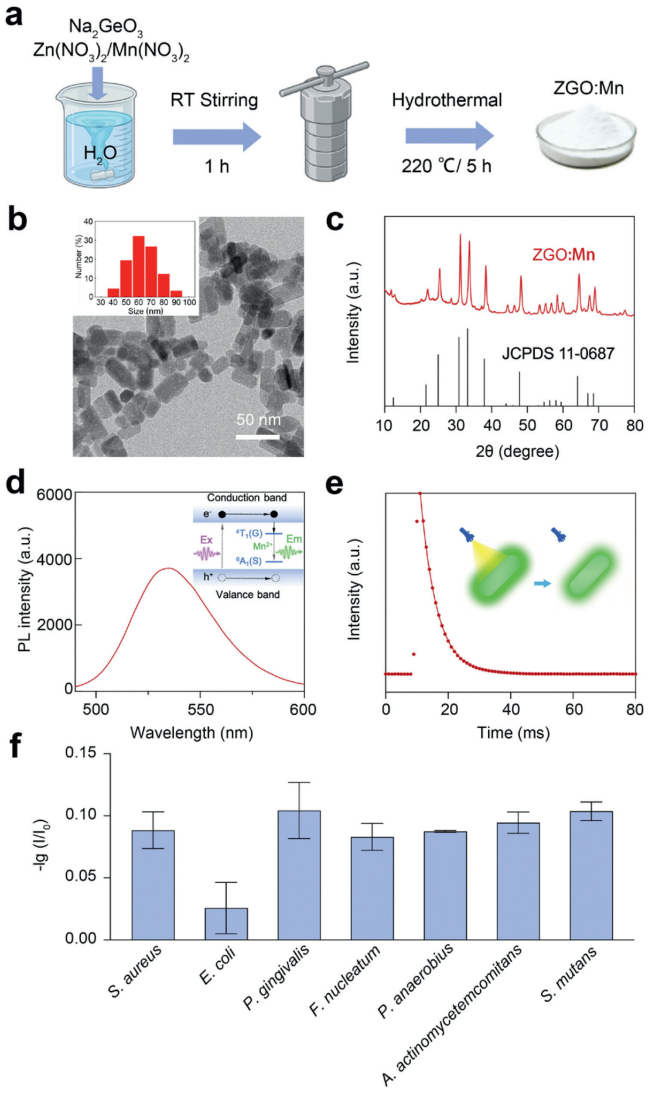

Fig. 1. (a) Schematic illustration of the synthesis of ZGO:Mn PLNPs. (b) TEM image of the prepared ZGO:Mn PLNPs (Inset: the size distribution of the ZGO:Mn PLNPs). (c) XRD pattern of the prepared ZGO:Mn PLNPs. (d) Phosphorescence spectrum of the ZGO:Mn PLNPs. (e) Transient decay curve of the ZGO:Mn PLNPs. (f) Response ($-\lg(I/I_0)$) patterns of ZGO:Mn PLNPs in the presence of different microorganisms ($OD_{600} = 0.1$) (responses are an average of six measurements and the error bars are the standard deviation).

cording to the previous reported hydrothermal method (Fig. 1a) [26,30]. The size and crystal structure of the ZGO:Mn nanorods were studied using transmission electron microscopy (TEM) and X-ray powder diffraction (XRD). TEM image in Fig. 1b shows that the ZGO:Mn nanorods are well-dispersed with uniform shape and size. As the inset figure demonstrates, the length of the ZGO:Mn nanorods is about 60 nm. XRD results in Fig. 1c indicate that the ZGO:Mn nanorods are highly crystalline with rhombohedral structure (ICPDS file number 11–0687) [45]. By collecting the persistent luminescence signal of ZGO:Mn nanorods, the auto-fluorescence interference from samples can be efficiently eliminated, thus enabling high sensitivity and signal-to-noise ratio (Figs. S1 and S2 in Supporting information). Subsequently, the persistent luminescence in ZGO:Mn nanorods was further investigated. As Fig. 1d shows, it can be observed that the persistent luminescence emission of the ZGO:Mn nanorods peaks at around 535 nm, which originates from the $^4T_1(G)-^6A_1(S)$ transition of Mn^{2+} luminescence center (Fig. S3 in Supporting information) [32]. Additionally, ac-

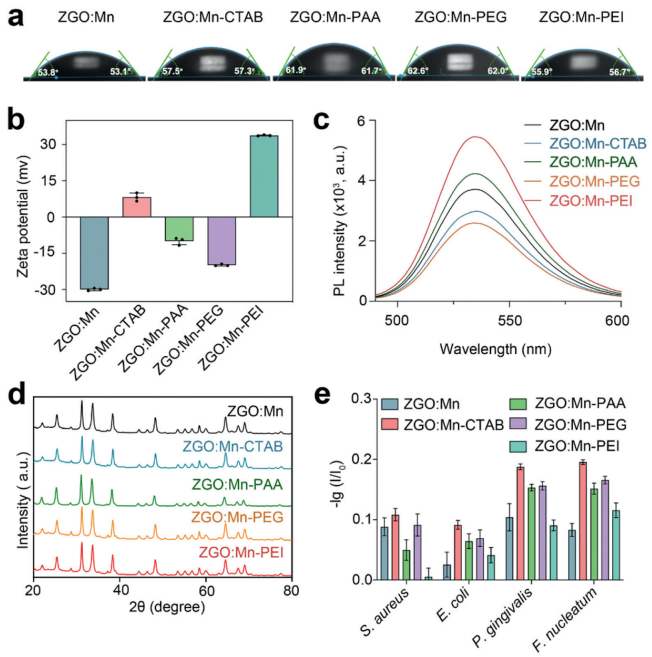

Fig. 2. (a) Optical images showing the contact angles and (b) Zeta potentials of the ZGO:Mn, ZGO:Mn-CTAB, ZGO:Mn-PAA, ZGO:Mn-PEG and ZGO:Mn-PEI droplets with a glass slide. (c) Phosphorescence spectrum and (d) XRD patterns of the ZGO:Mn, ZGO:Mn-CTAB, ZGO:Mn-PAA, ZGO:Mn-PEG and ZGO:Mn-PEI PLNPs. (e) Response ($-\lg(I/I_0)$) patterns of ZGO:Mn, ZGO:Mn-CTAB, ZGO:Mn-PAA, ZGO:Mn-PEG and ZGO:Mn-PEI PLNPs in the presence of different oral microorganisms ($OD_{600} = 0.1$) (responses are an average of six measurements and the error bars are the standard deviation).

cording to the transient decay curve (Fig. 1e), the photogenerated electron lifetime of the prepared ZGO:Mn nanorods was calculated to be 5.3 ms, clearly showing the existence of long-lived electrons in persistent luminescent ZGO:Mn nanorods. The results indicate that the ZGO:Mn PLNPs with persistent luminescence have been successfully prepared. After incubation with different bacteria, it can be seen that the persistent luminescence intensity varied differently (Fig. 1f). This can be owing to the distinguishing physical properties of the bacteria. The results suggest that ZGO:Mn PLNPs are applicable in bacteria differentiation.

Sensor arrays, called "electronic tongues", provide an alternative to time-consuming detection approaches [46]. Typically, sensor array-based detection of bacteria covers a variety of recognition mechanisms including the differences in physicochemical properties of bacteria such as charge and hydrophilicity. Based on the persistent luminescent ZGO:Mn nanorods, sensor arrays were further developed. Specifically, by modifying organic ligands with different charge and hydrophilicity properties including cetyl trimethyl ammonium bromide (CTAB), polyacrylic acid (PAA), polyethylene glycol (PEG) and polyethyleneimine (PEI) on the surface of ZGO:Mn nanorods, the arrayed one-component multichannel sensor was then obtained (Figs. S4 and S5 in Supporting information). As domenstrated in Fig. S6 (Supporting information), it can be observed that all the modified ZGO:Mn nanorods maintain the persistent luminescence. The contact angel images in Fig. 2a shows that the persistent luminescent nanoprobes have varied contact angel values ranging from 53° to 63°, suggesting the different hydrophilicities of the persistent luminescent nanoprobes (Fig. S7 in Supporting information). The zeta potential of the persistent luminescent nanoprobes in Fig. 2b demonstrate that the ZGO:Mn (−30.0 mV), ZGO:Mn-PAA (−10.0 mV) and ZGO:Mn-PEG (−19.9 mV) are negatively charged, while the ZGO:Mn-CTAB (8.2 mV) and ZGO:Mn-PEI (33.8 mV) are positively charged, indicating the different surface charges of theses persistent luminescent nanoprobes. In addition, it can be observed that the persistent luminescent nanoprobes have different persistent luminescent intensities as demonstrated in Fig. 2c. It can be observed that the phosphorescence intensity was shown as follows: ZGC:Mn-PEI > ZGC:Mn-PAA > ZGC:Mn > ZGC:Mn-CTAB > ZGC:Mn-PEG (Fig. S8 in Supporting information). The differing intensities might be owing to the reason that surface functional groups have influence on geometrical and electronic structures of ZGO:Mn, including the energy levels, energy gaps and the charge distribution [47]. The XRD results in Fig. 2d demonstrate that the structures are maintained after the surface modification. Accordingly, the persistent luminescent intensity variation can be ascribed to the surface modification. Subsequently, the feasibility of the obtained optical sensor array based on persistent luminescence was further explored. After the addition of bacteria, the persistent luminescent intensities were recorded. Taken the four bacteria including *S. aureus*, *E. coli*, *P. gingivalis*, *F. nucleatum* as examples, it can be seen that persistent luminescent intensities of each channel were significantly changed (Fig. 2e), potentially due to the non-specific interaction between the nanoprobes and the bacteria (Figs. S9 and S10 in Supporting information). Thus, we believe that the constructed sensor array based on persistent luminescence enables the efficient differentiation of oral bacterial strains.

To investigate the performance of the constructed sensor array based on persistent luminescence in identifying oral bacteria, 7 common strains were selected for testing as demonstrate in Table S1 (Supporting information) (Fig. 3a) [48,49]. After incubation with different bacteria at a concentration of $OD_{600} = 0.1$, the persistent luminescence intensities were recorded respectively. As the heat map in Fig. 3b shows, each channel in the sensor array exhibited distinctive response to the oral bacteria. In nature, bacteria are always existed as mixed cultures. Hence, we further test the ability of the constructed sensor array in discriminating and identifying bacterial mixtures. Herein, *E. coli* and *P. gingivalis* were used as the research model. A variety of *E. coli* and *P. gingivalis* ratios (100:0, 85:15, 50:50, 15:85 and 0:100) with the OD_{600} of 0.1 were incubated with the sensor array respectively. Similarly, after incubation, the persistent luminescence intensities were recorded. It can be seen that the persistent luminescence encoded sensor array also demonstrated differential phosphorescence responses to the ratios of mixed bacteria (Fig. 3c).

Consequently, a multivariate statistical analysis (linear discriminant analysis (LDA)) was performed. The canonical score LDA plots in Figs. 3d and e show that both the individual bacteria with the same species and the mixed bacteria with the same ratios were clearly classified into their corresponding categories by hierarchical clustering analysis. The above results demonstrate that oral bacteria could be well classified with the discrimination accuracy up to 100%, much higher than the accuracy by adopting three or four types of ZGO:Mn as demonstrated in Figs. S11 and S12 (Supporting information). Collectively, it can be concluded that this constructed sensor array based on persistent luminescent nanoprobes enables the efficient and precise differentiation of both the oral bacteria and the bacterial ratio mixture.

To further explore the practical clinical applications, the performance in discrimination of bacteria in artificial saliva samples are tested. According to the literature, the body fluid sample is typically identified positive when it contains > 10^5 cfu/mL (OD_{600} > 0.001) of bacteria. Herein, 7 oral bacteria with a concentration of $OD_{600} = 0.1$ was incubated with the above constructed sensor array in artificial saliva solution. Furthermore, a variety of *E. coli* and *P. gingivalis* ratios (100:0, 85:15, 50:50, 15:85 and 0:100) with OD_{600} of 0.1 were incubated with the sensor array respectively in artificial saliva solution. The persistent luminescence intensities were then recorded. As show in Figs. 4a and b, it can be observed that the

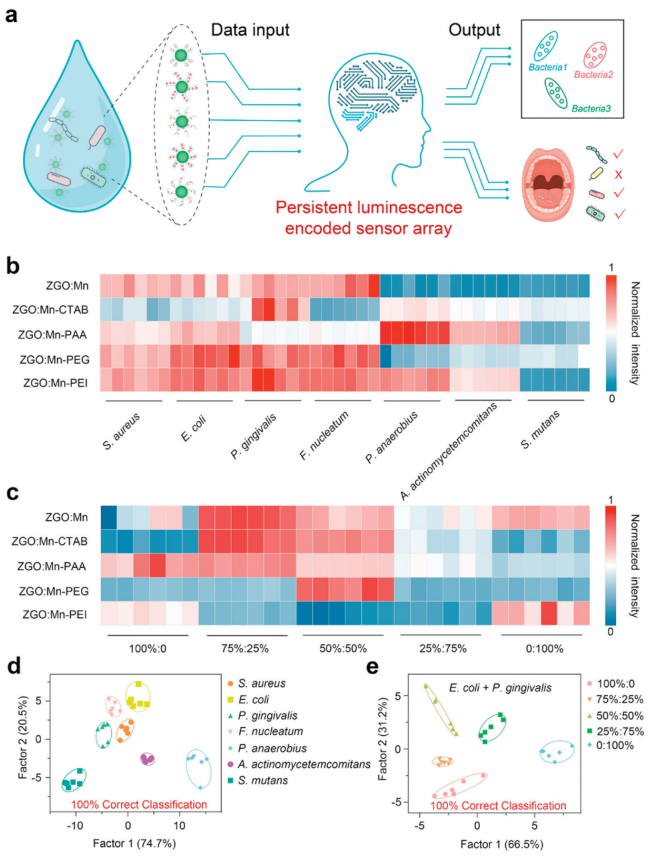

Fig. 3. (a) Schematic illustration for the oral microorganism identification with the persistent luminescence encoded array sensor. Heat map of the phosphorescence response of (b) oral microorganism and (c) the bacterial mixtures of *E. coli* and *P. gingivalis* with different ratios (normalized relative phosphorescence intensity change, $OD_{600} = 0.1$) in PBS solution. Six replicates are shown for each bacterium. (d) Canonical score plot for the response patterns as obtained from LDA. (e) LDA plot for the bacterial mixtures of *E. coli* and *P. gingivalis* with different ratios.

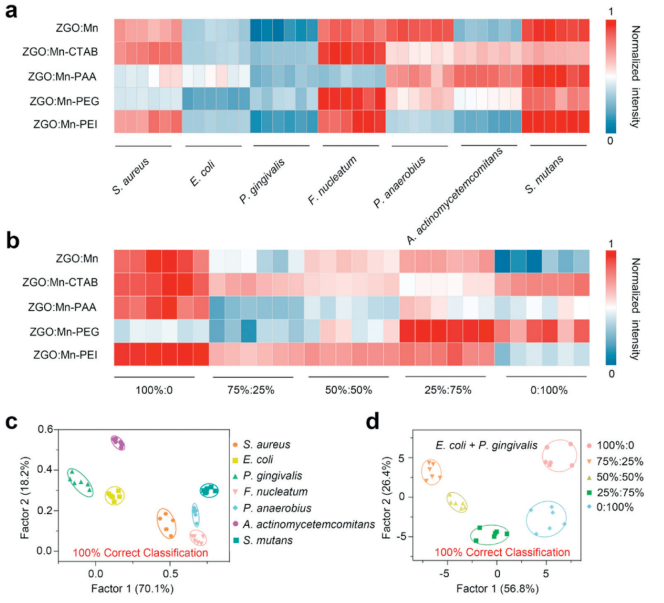

Fig. 4. Heat map of the phosphorescence response of (a) oral-derived microorganism and (b) the bacterial mixtures of *E. coli* and *P. gingivalis* with different ratios (normalized relative phosphorescence intensity change, $OD_{600} = 0.1$) in artificial saliva solution. Six replicates are shown for each bacterium. (c) Canonical score plot for the response patterns in artificial saliva solution as obtained from LDA. (d) LDA plot for the bacterial mixtures of *E. coli* and *P. gingivalis* with different ratios in artificial saliva solution.

persistent luminescence encoded sensor array both showed differential phosphorescence responses to the different oral bacteria species and the different ratios of mixed bacteria (Figs. S13 and S14 in Supporting information). As the canonical score LDA plots demonstrate in Figs. 4c and d, the oral bacteria with the same species and the mixed bacteria with the same ratios can be classified into their corresponding categories by hierarchical clustering analysis, indicating that the bacteria can be well classified with the constructed persistent luminescence encoded sensor array.

In summary, this paper presents a persistent luminescence-encoded multiple-channel optical sensing array which enables the rapid and accurate identification of oral-derived microorganisms within 30 min. Different persistent luminescent nanoprobes based on ZGO:Mn PLNPs including ZGO:Mn-CTAB, ZGO:Mn-PAA, ZGO:Mn-PEG and ZGO:Mn-PEI with distinct charges and hydrophilicity were prepared to construct the sensor array. With the constructed persistent luminescence-encoded optical sensor array, the microorganism was efficiently identified with the accuracy up to 100% both in PBS solution and artificial saliva samples. Furthermore, the persistent luminescence-encoded multiple-channel optical sensing array allows the detection of mixed bacteria with different ratio at low concentration ($OD_{600} = 0.1$) both in PBS solution and artificial saliva samples. The proposed sensor array in this work offers ideas for rapid and accurate oral-derived microorganism detection. In the future, we will continue to improve the persistent luminescence-encoded sensor array performance and develop point-of-care detection devices. By integrating with the smartphone, this work is expected to provide new ways for disease diagnosis associated with microbial metabolism, providing technical support for the development of smart healthcare.

Declaration of competing interest

The authors declare that they have no known competing financial interests or personal relationships that could have appeared to influence the work reported in this paper.

CRediT authorship contribution statement

Chaohui Zheng: Writing – original draft, Visualization, Validation, Investigation, Formal analysis. **Jing Xi:** Writing – original draft, Visualization, Validation, Investigation, Conceptualization. **Shiyi Long:** Visualization, Validation, Investigation. **Tianpei He:** Visualization, Validation. **Rui Zhao:** Validation, Investigation. **Xinyuan Luo:** Writing – review & editing. **Na Chen:** Writing – review & editing, Resources, Project administration, Formal analysis. **Quan Yuan:** Writing – review & editing, Resources, Project administration, Funding acquisition, Conceptualization.

Acknowledgments

This work was financially supported by Quanzhou high-level Talents Project Fund (No. 2022C033R), the National Natural Science Foundation of China (Nos. 21925401, 52221001), the Fundamental Research Funds for the Central Universities (No. 2042022rc0004), the Postdoctoral Innovative Research of Hubei Province of China (No. 211000025) and the interdisciplinary innovative talents foundation from Renmin Hospital of Wuhan University.

Supplementary materials

Supplementary material associated with this article can be found, in the online version, at doi:10.1016/j.cclet.2024.110223.

References

[1] G. Hajishengallis, T. Chavakis, Nat. Rev. Immunol. 21 (2021) 426–440.
[2] M. Freire, K.E. Nelson, A. Edlund, Trends Microbiol. 29 (2021) 551–561.
[3] M.L. Qi, X. Ren, W. Li, et al., Nano Today 43 (2022) 101447.
[4] L. Gao, T.S. Xu, G. Huang, et al., Protein Cell 9 (2018) 488–500.
[5] E. Read, M.A. Curtis, J.E. Neves, Nat. Rev. Gastro. Hepat. 18 (2021) 731–742.
[6] J. Pacheco-Yanes, E. Reynolds, J. Li, E. Mariño, Trends Mol. Med. 29 (2023) 912–925.
[7] Y.W. Lin, X.Y. Liang, Z.Y. Li, et al., Int. J. Oral Sci. 16 (2024) 2.
[8] X. Xiao, S.F. Liu, H. Deng, et al., Front. Microbiol. 14 (2023) 1121737.
[9] A. Nozawa, H. Oshima, N. Togawa, T. Nozaki, S. Murakami, PLoS One 15 (2020) e0229485.
[10] H.S. Na, S.Y. Kim, H. Han, et al., J. Clin. Med. 9 (2020) 1549.
[11] H.R. Liu, Z.H. Li, R.C. Shen, et al., Nano Lett. 21 (2021) 2854–2860.
[12] J. Wang, Z.R. Jiang, Y.R. Wei, et al., ACS Nano 16 (2022) 3300–3310.
[13] P. Wen, F. Yang, H.X. Zhao, et al., Anal. Chem. 96 (2024) 1454–1461.
[14] B.Y. Li, X.Z. Li, Y.H. Dong, et al., Anal. Chem. 89 (2017) 10639–10643.
[15] G.J. Liu, S.N. Tian, C.Y. Li, G.W. Xing, L. Zhou, ACS Appl. Mater. Inter. 9 (2017) 28331–28338.
[16] R. Nissler, O. Bader, M. Dohmen, et al., Nat. Commun. 11 (2020) 5995.
[17] L. Otten, E. Fullam, M.I. Gibson, Mol. Biosyst. 12 (2016) 341–344.
[18] W.W. Chen, Q.Z. Li, W.S. Zheng, et al., Angew. Chem. Int. Ed. 53 (2014) 13734–13739.
[19] G.W. Xing, W.F. Zhang, N. Li, et al., Chin. Chem. Lett. 33 (2022) 1743–1751.
[20] H. Wang, L. Zhou, J. Qin, et al., Anal. Chem. 94 (2022) 10291–10298.
[21] J.B. Tu, R.M. Torrente-Rodríguez, M.Q. Wang, W. Gao, Adv. Funct. Mater. 30 (2020) 1906713.
[22] S.M. Yoo, S.Y. Lee, Trends Biotechnol. 34 (2016) 7–25.
[23] B.A. Prabowo, R.Y.L. Wang, M.K. Secario, et al., Biosens. Bioelectron. 92 (2017) 186–191.
[24] J.Y. Yang, S.S. Lu, B. Chen, et al., Trac-Trend Anal. Chem. 159 (2023) 116945.
[25] B. Hu, J.W. Zhu, J.N. Shen, L. Yang, C.L. Jiang, Anal. Chem. 94 (2022) 7559–7566.
[26] H.B. Liang, Y.M. Wang, L. Zhang, et al., Sensor Actuat. B: Chem. 373 (2022) 132764.
[27] Y.Q. Zhang, Y. Liu, L.Y. Li, X.Q. Tao, E.Q. Song, Chin. Chem. Lett. 34 (2023) 108102.
[28] J. Wang, Q.Q. Ma, W. Zheng, et al., ACS Nano 11 (2017) 8185–8191.
[29] J. Wang, Q.Q. Ma, X.X. Hu, et al., ACS Nano 11 (2017) 8010–8017.
[30] Y.Q. Wang, Z.H. Li, Q.S. Lin, et al., ACS Sensors 4 (2019) 2124–2130.
[31] N. Chen, N. Du, R.C. Shen, et al., Nat. Commun. 14 (2023) 6800.
[32] N. Chen, N. Du, W.J. Wang, et al., Angew. Chem. Int. Ed. 61 (2022) e202115572.
[33] N. Chen, D. Cheng, T.P. He, Q. Yuan, Chin. J. Chem. 41 (2023) 1836–1840.
[34] O. Shelef, T. Kopp, R. Tannous, et al., J. Am. Chem. Soc. 146 (2024) 5263–5273.
[35] Y.P. Wu, X. Liu, Q.H. Wu, J. Yi, G.L. Zhang, Anal. Chem. 89 (2017) 7084–7089.
[36] W.L. Lu, X.Q. Chen, L. Wang, H.F. Li, Y.V. Fu, Anal. Chem. 92 (2020) 6288–6296.
[37] W.Y. Tang, Z.S. Chen, Z.L. Song, ACS Nano 16 (2022) 10968–10978.
[38] T. Yu, Y.L. Xianyu, Small 17 (2021) 2006230.
[39] K.L. Diehl, E.V. Anslyn, Chem. Soc. Rev. 42 (2013) 8596–8611.
[40] X.L. Yu, L.X. Fu, T. Wang, et al., Chin. Chem. Lett. 35 (2024) 109167.
[41] U. Farooq, Q.L. Yang, M.W. Ullah, S.Q. Wang, Biosens. Bioelectron. 118 (2018) 204–216.
[42] N. Chen, X.M. Zhang, J. Xi, Y.B. Yang, Q. Yuan, Sci. China Chem. 66 (2023) 2941–2950.
[43] L.L. Liang, J.Y. Chen, K. Shao, et al., Nat. Mater. 22 (2023) 289–304.
[44] P. Pei, Y. Chen, C.X. Sun, et al., Nat. Nanotechnol. 16 (2021) 1011–1018.
[45] V.Y. Suzuki, L.H.C. Amorin, N.M. Lima, et al., J. Mater. Chem. C 7 (2019) 8216–8225.
[46] X. Li, S.Q. Li, Q.Y. Liu, Z.B. Chen, Anal. Chem. 91 (2019) 6315–6320.
[47] J.K. Yu, X. Yong, Z.Y. Tang, S.Y. Lu, J. Phys. Chem. Lett. 12 (2021) 7671–7687.
[48] H. Min, K. Baek, A. Lee, Y. Seok, Y. Choi, J. Oral Microbiol. 13 (2021) 1905958.
[49] A.A.C. Satokata, J.H. Souza, L.L.O. Silva, et al., Anaerobe 76 (2022) 102588.